Templated Synthesis of Polymer-Based Yolk/Shell Particles with Tunable Morphologies Xuanrong Guo, Kiara Santiago González, and David M. Lynn^{1,2,*}

¹Department of Chemical and Biological Engineering, 1415 Engineering Drive, and ²Department of Chemistry, 1101 University Avenue, University of Wisconsin – Madison, Madison, Wisconsin 53706.

ABSTRACT: Polymer-based yolk/shell particles with functional components, including porous shells, removable shells, hollow cavities, or functional cores are of potential utility in many contexts. We report strategies for the synthesis of polymer-based yolk/shell particles templated by droplets of polymerizable oils contained within hollow and semi-permeable polymer capsules. Partial filling of degradable microcapsules with mixtures of vinyl monomers, followed by extraction into water, yielded yolk/shell-type structures composed of monomer droplets surrounded by larger polymeric shells. These encapsulated droplets can undergo changes in size (from micro- to nanoscale), shape (from spherical to lemon-like), and mobility upon exposure to different conditions and stimuli. Photo-polymerization of monomer droplets yielded crosslinked particle cores with morphologies templated by those of the liquid droplets, enabling the synthesis of various types of polymer yolk/shell structures. SEM images of polymer particle yolks after removal of surrounding capsules revealed spherical or lemon-like shapes with smooth morphologies. The aqueous environments within these yolk/shell structures can be used to host chemical reactions to further define and tailor particle properties. Thermal polymerization and subsequent crosslinking of poly(acrylic acid) yielded gels inside the capsules and a new 'hardboiled' yolk/shell morphology, with polymer cores imbedded in a solid, gel-like phase contained within a surrounding semi-permeable capsule.

Introduction

Microparticles and nanoparticles with yolk/shell structures—an architecture that typically comprises a movable core or 'yolk' encapsulated inside a hollow shell—have recently emerged as promising platforms for the design of composite colloidal materials. ¹⁻⁵ These yolk/shell particles have potential utility in a broad range of applications, ⁶⁻²⁴ including catalysis, ^{9, 15, 23} energy storage, ^{16, 20, 22} drug delivery, ^{11, 12} and biosensing. ^{10, 19} In contrast to conventional core/shell particles or hollow capsules, the structural complexity of yolk/shell particles provides additional opportunities for the integration of multiple functional elements into a single system. The three basic components of these materials (i.e., the movable core, polymer shell, and internal cavity) can each be individually designed, fabricated, and installed with different functionality and each of these components can act independently or synergically to address specific challenges. ¹⁻⁴ Past studies have demonstrated that, by exploiting a variety of building blocks and methods for the synthesis of these functional elements, the physical and chemical properties of yolk/shell particles, including electrical and optical properties, surface area, loading capacity, and chemical reactivity, can be conveniently manipulated and effectively tuned. ^{1-4, 6-20, 22, 23}

Many past studies have focused on the design and characterization of yolk/shell particles consisting of inorganic materials or hybrid materials composed of inorganic and polymer-based building blocks. 1-4, 6-20, 22, 23 Although yolk/shell particles with both polymeric shells and polymer-based cores are structurally and chemically interesting, they are relatively underexplored and relatively few approaches to the design of polymer yolk/shell particles have been reported in the literature. 25-32 Conventionally, polymer-based yolk/shell particles are often prepared using a two-step strategy, beginning with the fabrication of a multi-component core/shell structure, followed by the selective removal of intermediate sacrificial layers. 25-30 Past

studies have demonstrated that, when combined with distillation-precipitation polymerization and/or self-assembly approaches, different functional components, such as stimuli-responsive polymer materials and therapeutic payloads, can be incorporated into yolk/shell particles. 25-32 Thermo-responsive and pH-responsive polymer yolk/shell particles, for example, have been synthesized to deliver a model anticancer drug for tumor therapy. 30 A recent study also developed an emulsion-based approach to fabricate biocompatible silk fibroin yolk/shell particles that contained bone growth factor for improved hemostasis and bone repair. 32 Overall, these past studies demonstrate the potential utility of polymer-based yolk/shell particles and provide a basis for the development of new approaches to advanced functional colloidal systems.

Here, we report a facile approach to the design and fabrication of uniform, functionalizable polymer-based yolk/shell particles with tunable morphologies. Our approach exploits methods for the reactive layer-by-layer assembly of hollow microcapsules using poly(2-vinyl-4,4-dimethylazlactone) (PVDMA) and primary amine-containing linkers.³³⁻⁴¹ Past studies have demonstrated that the presence of residual azlactone reactivity in these multilayer assemblies provides opportunities for facile post-modification using various nucleophiles,^{33, 40} which provides convenient access to a broad range of functional films.³³⁻⁴¹ Additionally, the covalently crosslinked nature of these assemblies provides stability in a variety of environmental conditions.³³⁻⁴¹ We have demonstrated that non-degradable³⁴ or degradable⁴¹ amine-containing cross-linking components can be paired with PVDMA to fabricate hollow, semi-permeable microcapsules that are either stable³⁴ or degradable⁴¹ in aqueous media using a sacrificial core-templated approach. Of particular relevance to this study, we recently reported that hollow microcapsules fabricated using PVDMA and the primary amine-containing polymer branched poly(ethylenimine) (PEI) could be filled, post-fabrication, with liquid crystals, a class of stimuli-

responsive liquid materials.³⁷⁻³⁹ That approach yielded spherical polymer shells that were partially-filled with smaller spherical LC droplets, a stimuli-responsive yolk/shell-type structure that we refer to as 'caged' LC droplets.³⁷

The work reported here sought to exploit that approach to develop new strategies for the synthesis of polymer yolk/shell particles with different morphologies, including solid micro- and nanoparticle yolks of varying size and shape. This overall approach differs significantly from past approaches to the fabrication of polymer yolk/shell particles from core/shell structures, as it utilizes swelling of the polymer shells in aqueous media to create interstitial void spaces.³⁷⁻³⁹ We first demonstrate proof-of-concept using reductively degradable capsules partially-filled with a simple alkane, tetradecane, and then demonstrate approaches to the design of solid yolks using isotropic mixtures of photo-polymerizable vinyl monomers as model reactive oils. Our results reveal that filling of monodisperse porous microcapsules with hydrophobic liquids yields partially-filled, yolk/shell-type structures with uniform sizes and morphologies, and that photopolymerization of reactive liquid monomers contained in partially-filled microcapsules leads to solid polymer particles inside the polymer shells. We further demonstrate that, by control over the wetting and diffusion properties of monomer droplets prior to polymerization, it is possible to tune key features of the encapsulated polymer particles, such as their shapes (spherical or lemonlike), sizes (micro- or nanoscale), and the mobility of the polymer cores. Finally, we explore the potential of these semi-permeable yolk/shell particles to host chemical reactions. As proof-ofconcept, we demonstrate that the aqueous void space in these yolk/shell particles can be used as a reaction chamber for the synthesis of polymer hydrogels. These approaches provide methods for the synthesis of polymer-based particles with anisotropic shapes, internal morphologies, and properties that would be difficult to access using other methods.

Materials and Methods

Materials. Cystamine dihydrochloride, tetradecane, hexadecane, pyrene, 2,2'-azoisobutyronitrile (AIBN), potassium peroxodisulfate (KPS), 2,2-dimethoxy-2-phenylacetophenone (DMPAP), dodecyltrimethylammonium bromide (DTAB), sodium dodecyl sulfate (SDS), 1,6-hexanediol dimethacrylate, acetic acid, sodium hydroxide, acetonitrile, zinc acetate dihydrate, and tetrahydrofuran (THF) were obtained from Sigma-Aldrich (Milwaukee, WI). Benzyl methacrylate was purchased from Scientific Polymer Products (Ontario, NY). Acrylic acid (99.5%) and 3-dimethylaminopropylamine (DMAPA) were purchased from Acros Organics (New Jersey, USA). 1,4-Dithiothreitol (DTT) was purchased from DOT Scientific (Burton, MI). Ethanol was obtained from Decon Labs. 2-Vinyl-4,4-dimethylazlactone (VDMA) was a kind gift from Dr. Steven M. Heilmann (3M Corporation, Minneapolis, MN). Poly(2-vinyl-4,4dimethylazlactone) (PVDMA, $M_W \sim 44,667$; D = 5.7) was synthesized by the free-radical polymerization of VDMA, as described previously. 40 Tetramethylrhodamine (TMR) cadaverine was obtained from Setareh Biotech (Eugene, OR). PVDMA labeled with TMR (1 mol%; referred to from hereon as PVDMA_{TMR}) was synthesized as described previously. 40 Cystamine free base (Cys) was prepared by deprotection of cystamine dihydrochloride using a previously reported protocol.⁴¹ Deionization of a distilled water source was performed using a Milli-Q system (Millipore, Bedford, MA) yielding water with a resistivity of 18.2 M Ω . FluoroDishTM confocal dishes were obtained from World Precision Instruments (Sarasota, FL). Glass microscope coverslips (22 CIR-1) were obtained from Fisher Scientific (Pittsburgh, PA). SiO₂ microparticles (average diameter = 5.04 µm) were purchased from Bangs Laboratories (Fishers, IN). All materials were used as received without further purification unless otherwise noted.

General Considerations. SiO₂ microparticles used as substrates for layer-by-layer assembly were rinsed with acetonitrile prior to use. Bright-field and fluorescence microscopy images were acquired using an Olympus IX70 inverted microscope (Center Valley, PA) using a 60X oil-immersion objective lens and analyzed using the Metavue version 4.6 software package (Universal Imaging Corporation). Scanning electron micrographs (SEM) were acquired using a LEO 1550VP Field Emission SEM (Königsallee, Göttingen, Germany). Samples were coated with a thin layer of gold using a sputterer (60 s at 10 mA, 500V, 70 mTorr) prior to imaging.

Fabrication of Microcapsules. Multilayer hollow microcapsules were prepared in analogy to previous reports.⁴¹ Briefly, solutions of PVDMA (or PVDMA_{TMR}; 20 mM with respect to the molecular weight of the polymer repeat unit) and the diamine crosslinker Cys (10 mM, also containing an equimolar amount of DMAPA) were prepared in acetonitrile. SiO₂ microparticles were placed into plastic microcentrifuge tubes and suspended in 1 mL of acetonitrile to wash the microparticles prior to multilayer assembly. The first layer of Cys was deposited onto the SiO₂ particles by adding 1 mL of the Cys solution to the particle suspension and manually shaking the particles for 1 minute to allow sufficient time for the polymer to adsorb to the particle surface. The particles were then centrifuged for 1 minute at 1500 rpm. The supernatant was then carefully removed by pipette and the particles were rinsed two times by resuspending them in 1 mL of acetonitrile and vortexing. After each rinse in acetonitrile, the particles were centrifuged for 1 minute at 1500 rpm and the supernatant was removed. The second layer of the multilayered film was then deposited by adding 1 mL of PVDMA solution to the particle suspension and shaking manually for 30 seconds. The particles were then rinsed two times with 1 mL of acetonitrile as

described above. Subsequent layers were fabricated by repeating this process (by alternately depositing Cys or PVDMA solutions and allowing each layer to react for 30 seconds) until the desired number of polymer Cys/PVDMA layer pairs (or 'bilayers', typically four) were deposited onto the particle surface. After every two bilayers, particles were placed into a new microcentrifuge tube to minimize aggregation. After film fabrication, the coated particles were placed into 1 mL of 3-dimethylaminopropylamine in acetonitrile (40 mM) and shaken on an automated shaker plate for 1 hr to exhaustively react with all remaining azlactone functional groups and install tertiary amine functionality. Coated particles were then rinsed with acetonitrile three times, dispersed in 1 mL of deionized water, and then treated with hydrofluoric acid (HF, 5 M) for 10 minutes to etch away the silica cores [WARNING: HF solutions and vapors are extremely poisonous and corrosive, and may cause extreme burns that are not immediately painful! Handle with extreme caution, in a chemical fume hood, and using appropriate protective equipment (gloves, face/eye protection, lab coat, etc.), and neutralize waste appropriately. Do not store in glass containers.]. The resulting empty polymer capsules were washed, centrifuged, and re-suspended five times using water and characterized using bright-field microscopy.

Encapsulation of Hydrophobic Oils in Polymer Microcapsules. Empty capsules were rinsed and washed with ethanol twice and centrifuged down into a pellet. Droplets of hydrophobic oils were encapsulated in the microcapsules using a previously described procedure.³⁷ Briefly, the pellet in the microcentrifuge tube was washed with acetone once and suspended in 10 μL of acetone (~10⁶ particles/μL). A non-reactive hydrophobic oil, tetradecane (40 μL) was then added and the resulting mixture was placed on an automated shaker plate at room temperature for 15 hr in a closed container. After 15 hr, the microcentrifuge tube was uncapped and left open for 24 hr

to allow the solvent to evaporate. Excess tetradecane was removed by centrifugation and the remaining oil-filled capsules were extracted into DI water with gentle shaking. Reactive hydrophobic monomers were encapsulated by suspending the pellets of empty capsules in a solution of the photoinitiator DMPAP (3 mg DMPAP dissolved in 12 μ L ethanol or 2 mg/mL ethanol solution of pyrene, see text), followed by addition of benzyl methacrylate (45 μ L) and 1,6-hexanediol dimethacrylate (15 μ L). The process described above was then repeated to extract the monomer-filled capsules into an aqueous phase.

Characterization of Oil-Filled Microcapsules. A 20 μ L dispersion of oil-filled capsules was placed onto a glass coverslip and the capsules were allowed to settle and attach loosely through physical interactions to the surface for \sim 1 min in order to facilitate characterization by microscopy. Experiments to investigate the response of monomer-filled capsules to the addition of surfactants were performed by adding concentrated solutions of DTAB or SDS to the dispersion of capsules to achieve desired final concentrations. These capsules were allowed to settle and attach through physical interactions to the glass surface for \sim 15 min and changes in the shapes and motions of encapsulated oil droplets were characterized by bright-field and fluorescence microscopy. For experiments designed to control the sizes of encapsulated oil droplets, a hydrophobic oil, hexadecane, was used to leach loaded monomers. Hexadecane (200 μ L) was added to a 200 μ L dispersion of monomer-filled capsules in a fluorodish, and changes in the sizes of encapsulated oil droplets over time were recorded using video microscopy.

Polymerization and Characterization of Polymerized Particles. A dispersion of monomerfilled capsules (150 μL) was dispensed into a confocal dish and covered by a round glass coverslip. The monomer-filled capsules were cured in an XL-1500 UV Crosslinker (Spectronics Corporation) using 365 nm UV illumination for 10 min,^{43, 44} yielding solid polymer particles inside the capsules. Unreacted monomer was removed by rinsing with ethanol. The capsules were then re-suspended in DI water by sonication, immobilized onto glass coverslips as described above, and characterized using bright-field and fluorescence microscopy. For experiments designed to prepare bare polymer particles without capsules, the yolk/shell particles were re-suspended in aqueous solutions of DTT (10 mM) three times (10 min for each exposure) to remove the multilayer capsules.⁴¹ The resulting bare polymer particles were washed three times with DI water and characterized using bright-field and fluorescence microscopy. Samples for SEM imaging were prepared by placing a 1 µL dispersion of polymerized particles (with or without capsules) onto a silicon chip, followed by removal of water under vacuum and subsequently coating with a thin layer of gold.

Preparation of Poly(Acrylic Acid) Gels in Microcapsules. Monomer-filled capsules were first polymerized using UV exposure, and then immobilized onto glass slides as described above. Briefly, a 20 μL dispersion of the yolk/shell particles was placed on a glass slide and allowed to settle for a period of ~15 min under humid conditions. The surface was then rinsed by flowing DI water over it using a micropipette at a rate of approximately 200 μL/s for 1 min to remove unattached or loosely bound particles. The glass slide with immobilized yolk/shell particles was then immersed into a 24 mL glass vial containing a 1.0 M aqueous solution of acrylic acid (with 0.013 M KPS). Free radical polymerization of acrylic acid was performed in an oil bath at 70 °C for 30 min. 45-47 The glass slide was then removed from the vial and washed with 0.02 M NaOH followed by DI water. Immobilized yolk/shell particles were characterized using bright-field

microscopy. For experiments designed to induce gelation inside capsules, immobilized yolk/shell particles containing PAA were washed with HAc/NaAc buffer (pH = 5). A 100 mM solution of $Zn(Ac)_2$ (pH = 5) was then added and changes in the morphology of the yolk/shell particles were observed using bright-field microscopy.

Results and Discussion

Fabrication and Characterization of Hollow Microcapsules Partially-Filled with a Model Isotropic Oil

In past studies, we demonstrated that anisotropic thermotropic liquid crystals (LCs) could be loaded/infused into hollow microcapsules fabricated by the reactive layer-by-layer assembly of the amine-reactive polymer PVDMA (polymer 1, Figure 1A) and the non-degradable polyamine PEI using a sacrificial template approach.³⁷⁻³⁹ That approach led to partially-filled capsules with yolk/shell-type structures that were stable in aqueous media. Those studies also demonstrated that these 'caged' LC structures could undergo changes in shape and rotational mobility upon exposure to aqueous amphiphiles that are not observed using conventional 'bare' LC emulsion droplets or empty capsules.³⁷⁻³⁹ These and other interesting features of these materials motivated us to explore the potential of this approach for the development of new types of polymer-based yolk/shell systems.

In this study, we sought to explore the generality of this post-loading and capsule-swelling approach using a new class of reductively degradable microcapsules (shown schematically in Figure 1B) and different isotropic oils, including nonreactive and photopolymerizable oils, to fabricate yolk/shell particles with solid or liquid yolks and various morphologies and functional properties. Reductively degradable capsules were prepared by the template–assisted approach described above, using monodisperse silica templates ($5.2 \pm 0.2 \mu m$ in diameter, measured from optical micrographs using ImageJ, see Figure S1), PVDMA, and a disulfide-containing diamine linker cystamine (Cys, linker 2, Figure 1A) as building blocks.⁴¹ Based on our past studies, a monofunctional amine, 3-dimethylaminopropylamine (DMAPA, linker 3, Figure 1A), was also included as a building block during assembly to tune the swelling

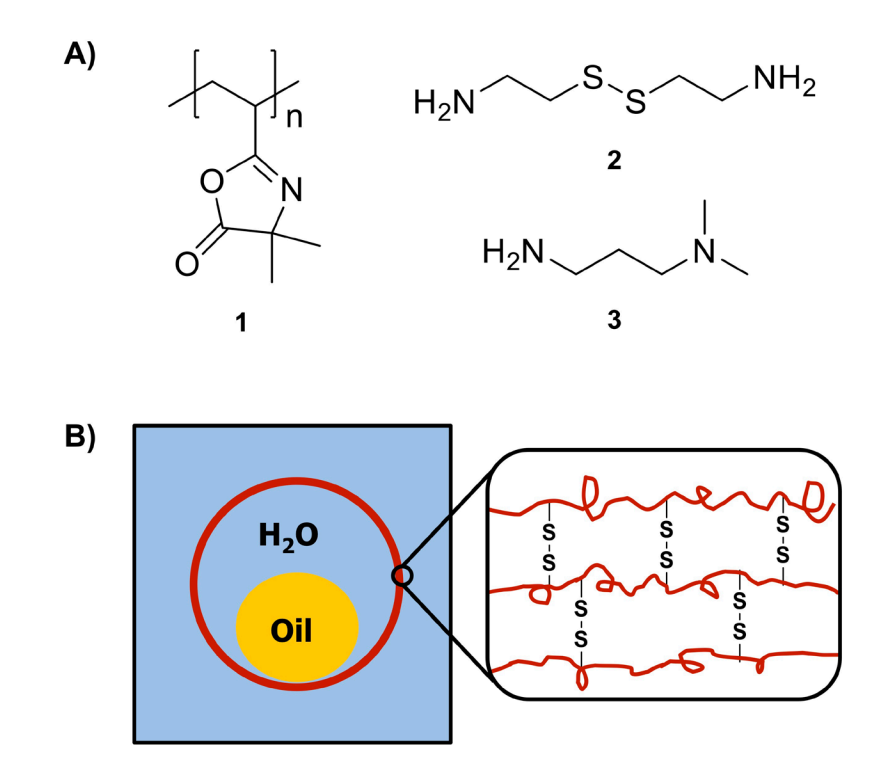


Figure 1: (A) Chemical structures of the azlactone-containing polymer **1** (PVDMA), disulfide-containing diamine linker **2** (Cys), and monofunctional amine **3** (DMAPA) used in this study. (B) Schematic illustration showing a disulfide crosslinked, multilayer PVDMA/Cys capsule (red) containing a droplet of oil (yellow) suspended in water (blue).

and degradation behaviors of the capsules (an equal molar amount of DMAPA with respect to Cys was used in linker dipping solutions, and the assembled azlactone-containing multilayers were treated with DMAPA prior to removal of the template; see Materials and Methods and past studies⁴¹ for additional information and discussion of this procedure).

Subsequent etching of multilayer-coated silica templates with HF yielded hollow capsules (Figure 2A) functionalized with hydrophilic tertiary amine groups.⁴¹ These hollow capsules were then infused with tetradecane, a model isotropic oil, followed by the extraction of the oil-filled capsules into deionized water. This process resulted in free-floating microcapsules containing smaller oil droplets with lemon-like shapes (Figure 2B). This yolk/shell morphology is similar to that observed in our past studies of 'caged' LC droplets in PEI/PVDMA capsules,³⁷⁻³⁹ and arises from the swelling of the polymer microcapsule when the oil-filled capsules are extracted into water. Inspection of hollow capsules in water reveals a diameter of approximately $11.3 \pm 0.6 \,\mu m$ (Figure 2A). However, when these capsules were dispersed in tetradecane, their size decreased down to $6.7 \pm 0.3 \,\mu m$ in diameter (Figure S1). Upon extraction of the capsules from tetradecane into another aqueous phase, the polymer capsules returned to a size of $11.3 \pm 1.00 \,\mu m$

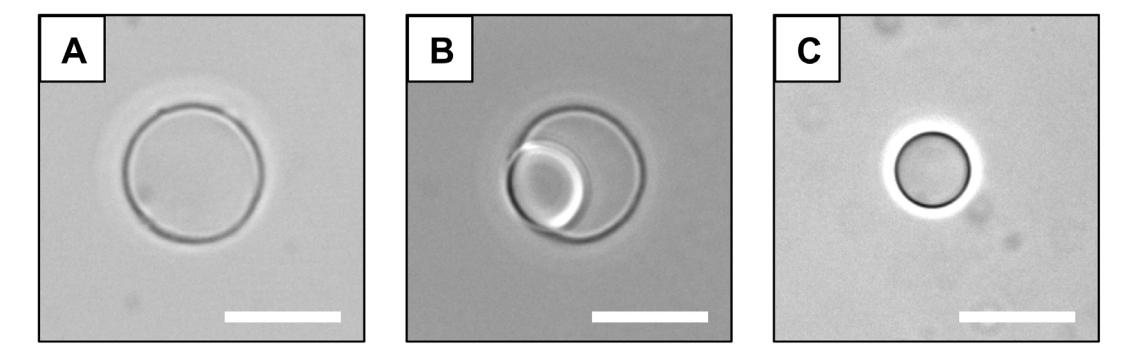


Figure 2: Bright-field microscopy images showing a PVDMA/Cys capsule (A) before and (B) after filling with tetradecane (the capsule is shown suspended in deionized water), and (C) an emulsion droplet of tetradecane after removal of its surrounding PVDMA/Cys capsule by addition of 10 mM DTT. Scale bars are 10 μm.

 $0.6~\mu m$ in diameter (Figure 2B), resulting in a yolk/shell-type structure in which a larger polymer membrane 'shell' surrounds a smaller oil droplet 'yolk'. These partially-filled capsules were stable in water, but they dissolved rapidly (in a few seconds) upon exposure to reducing agents such as DTT (10~mM), releasing free-floating spherical droplets of oil with sizes of $6.3\pm0.5~\mu m$ in diameter (Figure 2C) that were dictated by the sizes of capsules in the oil phase during loading. This stimuli-responsive behavior is also consistent with our past studies on the characterization of empty PVDMA/Cys microcapsules, 41 and occurs as a result of the cleavage of the disulfide bonds that form in these assemblies during fabrication. In principle, the volume ratio of these yolk/shell-type capsules could be tuned by control over the swelling behaviors of PVDMA/Cys capsules, such as by varying the molar ratio of DMAPA during fabrication 41 or by changing the solvent properties of the oil phase during loading. $^{37-39}$

Fabrication and Characterization of Yolk/Shell Structures Containing Solid Polymer-Based Yolks

We reasoned that the above approach to the partial-filling of PVDMA/Cys capsules could be used in combination with polymerizable hydrophobic liquid monomer oils to design new types of polymer-based yolk/shell particles containing solid polymeric yolks. For these experiments, we used an acrylate monomer, benzyl methacrylate (BzMA), containing 20 wt % of the diacrylate crosslinker 1,6-hexanediol dimethycrylate (HDODA). To demonstrate the potential to install different functionalities into this system and assist with characterization using microscopy, we also doped the reactive oils with pyrene, a model hydrophobic fluorescent dye and fabricated polymer capsules using fluorescently labeled PVDMA (PVDMA_{TMR}). As shown in Figure 3A, this approach yielded uniform, yolk/shell-type capsules, with droplets of oil approximately $5.4 \pm 0.2 \, \mu m$ in diameter (defined by the size of the capsules suspended in

monomer as described above, see Figure S1) surrounded by larger capsules ($11.3 \pm 0.6 \mu m$ in diameter). These encapsulated droplets appeared spherical and displayed higher contact angles at oil/capsule wall interfaces than those of the droplets of tetradecane discussed above (e.g., see Figure 2B). These differences likely arise from differences in the interfacial tensions of the two oil species.

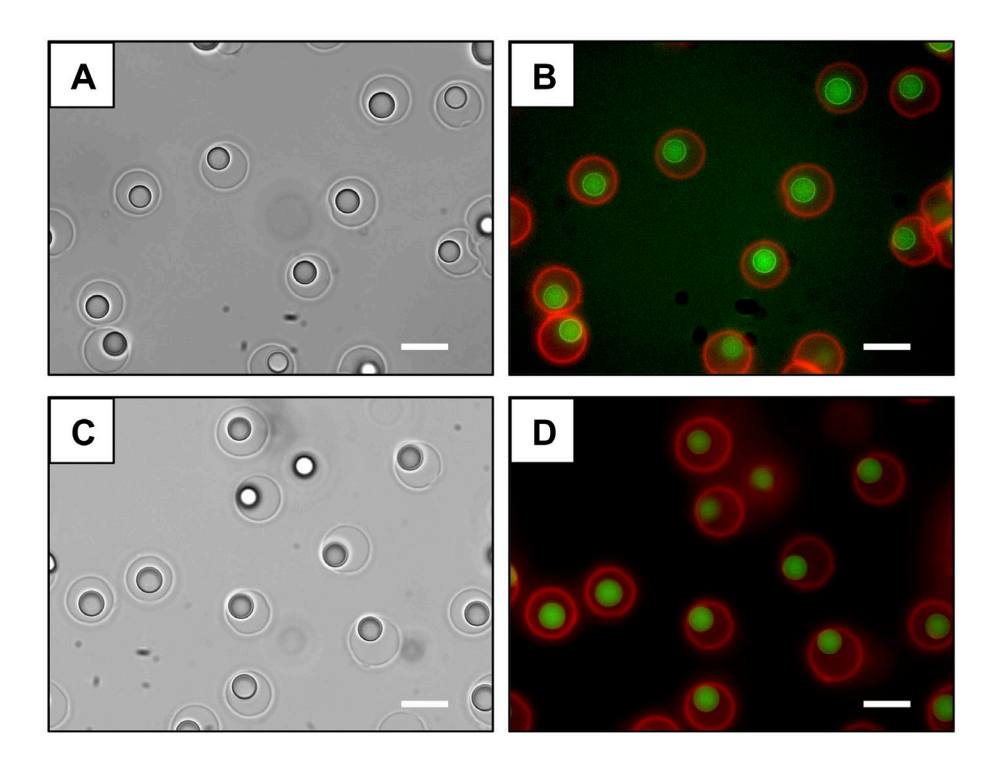


Figure 3: Bright-field and fluorescence microscopy images showing (A-B) monomer droplet-filled PVDMA_{TMR}/Cys capsules suspended in deionized water and (C-D) the corresponding polymer yolk/shell particles after UV illumination. The capsules (labeled with TMR-cadeverine) are false-colored red and the droplets or particles (containing pyrene) are false-colored green. Scale bars are $10 \, \mu m$.

Inspection of the corresponding fluorescence microscopy image (Figure 3B) reveals fluorescence signals associated with the pyrene loaded in the oil droplets (false-colored green) and TMR-cadaverine associated with labeled polymer capsules (false-colored red). The introduction of these loaded fluorophores did not result in measurable changes in the sizes or

shapes of these capsules, as evidenced by images of unlabeled capsules filled with pristine monomer mixtures that did not contain pyrene (Figure S2). Subsequent exposure of dispersions of these oil-filled capsules to UV illumination yielded polymer yolk/shell particles with solid polymer yolks (Figure 3C). The sizes of encapsulated yolks $(5.3 \pm 0.3 \, \mu \text{m})$ in diameter) were indistinguishable from those of the liquid droplets prior to polymerization. Fluorescence microscopy images (Figure 3D) further confirmed the presence of fluorophores in these polymer particles, demonstrating the potential to incorporate functional components into the yolks in these assemblies. These experiments demonstrate that the shapes of the reactive oil droplets, as well as the payloads within the droplets, can be 'locked' *in situ* by photo-polymerization, yielding polymer yolk/shell particles templated on the original oil-filled capsules.

Past studies demonstrated that surfactants can diffuse through semi-permeable PVDMA/PEI-based capsules and adsorb at 'caged' oil-aqueous interfaces, triggering changes such as wetting transitions of the encapsulated droplets. 37-39 Inspired by these studies, we

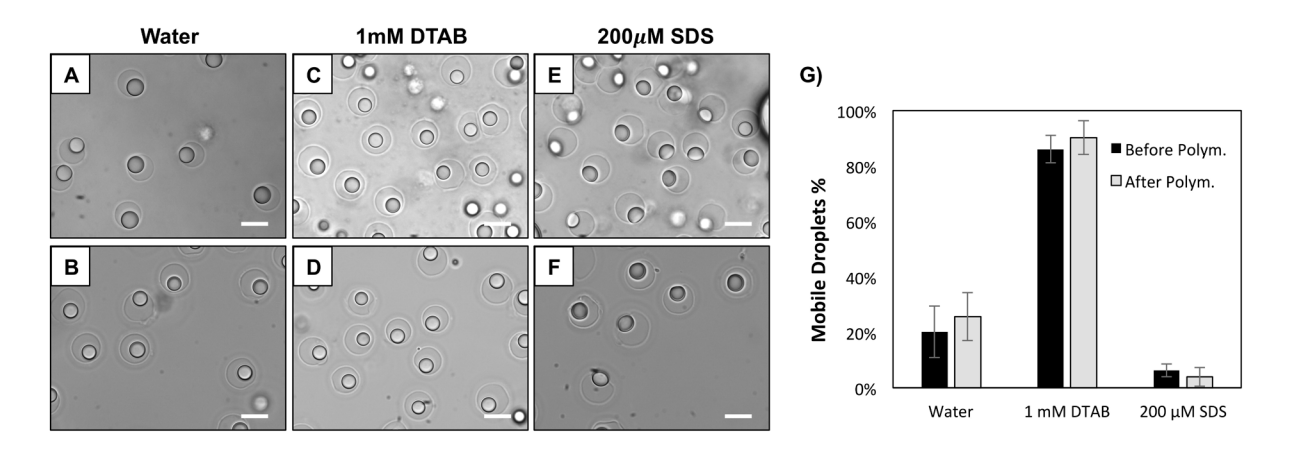


Figure 4: Bright-field images showing monomer droplet-filled PVDMA_{TMR}/Cys capsules suspended in different solutions (top row, A, C, E) and the corresponding polymer yolk/shell particles after UV illumination (bottom row, B, D, F). Monomer-filled capsules were incubated and polymerized in deionized water (A-B), in 1 mM DTAB (C-D), and in 200 μ M SDS (E-F). (G) Plot showing the percentages of mobile droplets (black) or polymer particles (grey) inside capsules under different conditions. Scale bars are 10 μ m.

performed a series of experiments to investigate the influence of model surfactants on oil droplets encapsulated in these PVDMA/Cys yolk/shell structures. To facilitate the characterization of loaded droplets/particles by microscopy, free-floating yolk/shell-type capsules used in the studies above were allowed to settle onto negatively charged bare glass coverslips (because these capsules were functionalized with cationic surface functionality, this resulted in reversible immobilization through electrostatic interactions;³⁹ see Materials and Methods). Characterization of surface-immobilized capsules incubated in deionized water revealed that the majority of the nearly spherical liquid monomer droplets resided at one side of the capsules and remained immobile inside the surrounding capsule; only $\sim 20 \pm 9\%$ of droplets were observed to translate or rotate inside the capsules (Figure 4A, G; Video S1), as evidenced by changes in their positions (caused by translation) or optical appearances (caused by water flow-induced rotation) of droplets under video microscopy. However, when a model cationic surfactant, dodecyltrimethylammonium bromide (DTAB, 1 mM) was added, 86 ± 5% of the droplets were observed to translate and rotate inside capsules, while retaining their spherical shapes (Figure 4C, G; Video S2), yielding yolk/shell structures containing freely-moving cores. In contrast, addition of the anionic surfactant sodium dodecyl sulfate (SDS, 200 µM) led to a significant decrease in apparent contact angles at oil/capsule wall interfaces, triggering transformations in droplet shapes from spherical (Figure 4A) to lemon-like (Figure 4E). The lemon-like droplets wetted the inner surfaces of the capsule and were mostly immobile (only ~6 \pm 2% of droplets were observed to translate or rotate, see Figure 4E, G; Video S3). These results, when combined, suggest that different surfactants can pass through the capsule wall of the degradable PVDMA/Cys capsules and induce changes in shape and/or mobility of encapsulated oil droplets in ways similar to those previously reported for 'caged' LC droplets in nondegradable PVDMA/PEI capsules.³⁷⁻³⁹

Additional experiments demonstrated that these reactive oil droplets could be subsequently polymerized in the presence of surfactants, and that the size and shape of yolk/shell structures remained almost unchanged after UV illumination (Figure 4B, D, and F). These results reveal a straightforward approach to the templated synthesis of polymer yolk/shell particles with shapes that mimic those of oil-filled capsules prior to polymerization. In addition, the mobility of the resulting solid polymer yolks was similar to those of their oil droplet counterparts prior to polymerization (Figure 4G; Video S1, S2 and S3). For example, polymerization in the presence of DTAB resulted in polymer capsules containing solid yolks that were also freely translating and rotating. The ability to control shape and mobility of polymer yolk/shell particles demonstrated here allows easy access to complex structures that can be difficult to achieve using other methods.

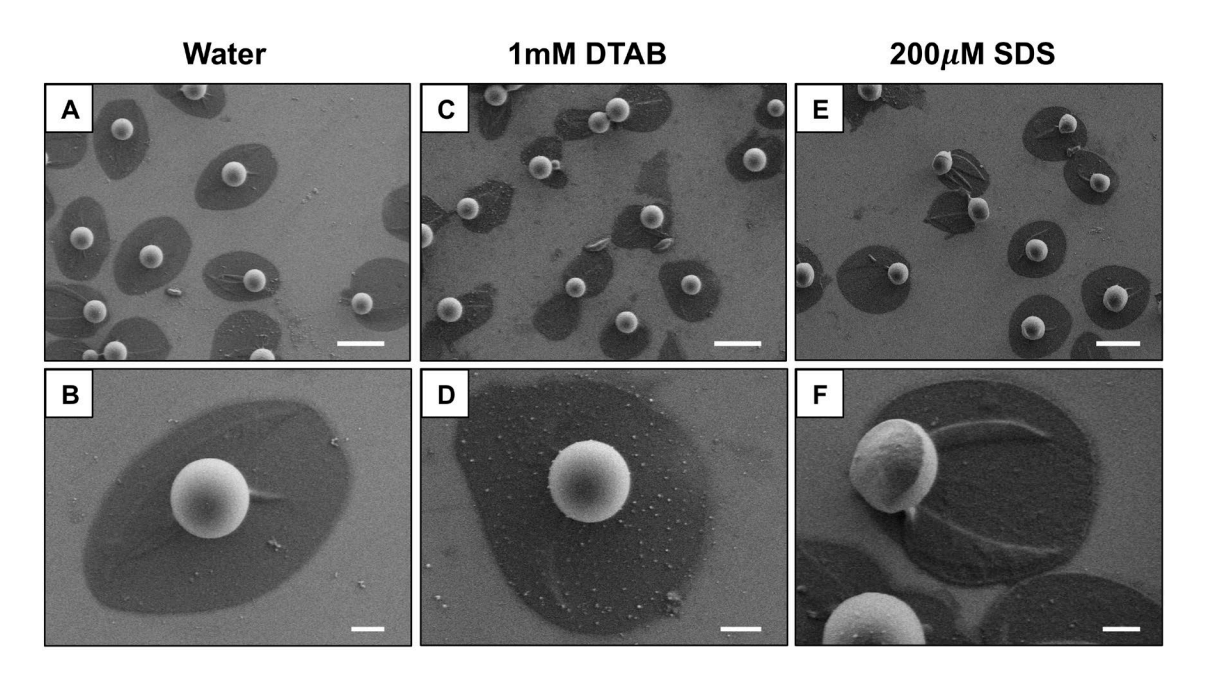


Figure 5: Representative low magnification (top row) and high magnification (bottom row) SEM images showing dried yolk/shell particles polymerized under different conditions. Images show yolk/shell particles polymerized (A-B) in deionized water, (C-D) in 1 mM DTAB, and (E-F) in 200 μ M SDS. Scale bars are 10 μ m (top row) and 2 μ m (bottom row), respectively.

Finally, we also characterized the shapes and structures of our polymerized yolk/shell particles using scanning electron microscopy (SEM). For these experiments, polymer yolk/shell particles were deposited onto silicon substrates from aqueous dispersions and dried in a vacuum desiccator prior to analysis. As shown in Figure 5, polymer particles were observed to colocalize with flattened, folded polymer capsules; few free particles (without surrounding polymer films) or hollow capsules (without associated particles) were observed in these experiments. No evidence of pores, cracks, or broken capsules was observed at the micrometer scale, suggesting the capsules remained intact upon drying. Overall, these results are consistent with the presence of solid polymer particles wrapped nearly conformly by the capsule wall upon drying. Since the polymer capsules conformed tightly to the surface of the particles inside, these images also reveal information about the shape and morphology of the encapsulated yolks. Inspection of Figure 5A-D revealed that particles polymerized in water or DTAB were nearly spherical, in contrast to the lemon-like shape of particles synthesized in the presence of SDS (Figure 5E-F). These results are consistent with our observations of yolk/shell particles using optical microscopy.

To provide additional insights into the shapes and surface morphologies of the encapsulated polymer yolk particles, we removed the degradable polymer capsules surrounding them by treatment with DTT. Panels A-C, D-F, and G-I of Figure 6 show optical and SEM images of the three types of polymer particles polymerized in water, DTAB, or SDS solutions, respectively, after DTT treatment. Residual polymer films and broken pieces of capsules were not observed in these images, suggesting complete removal of the reductively degradable polymer shells. The shell-free polymer particles appear to be relatively uniform in size, and demonstrate shapes that are similar to those of corresponding encapsulated particles observed in

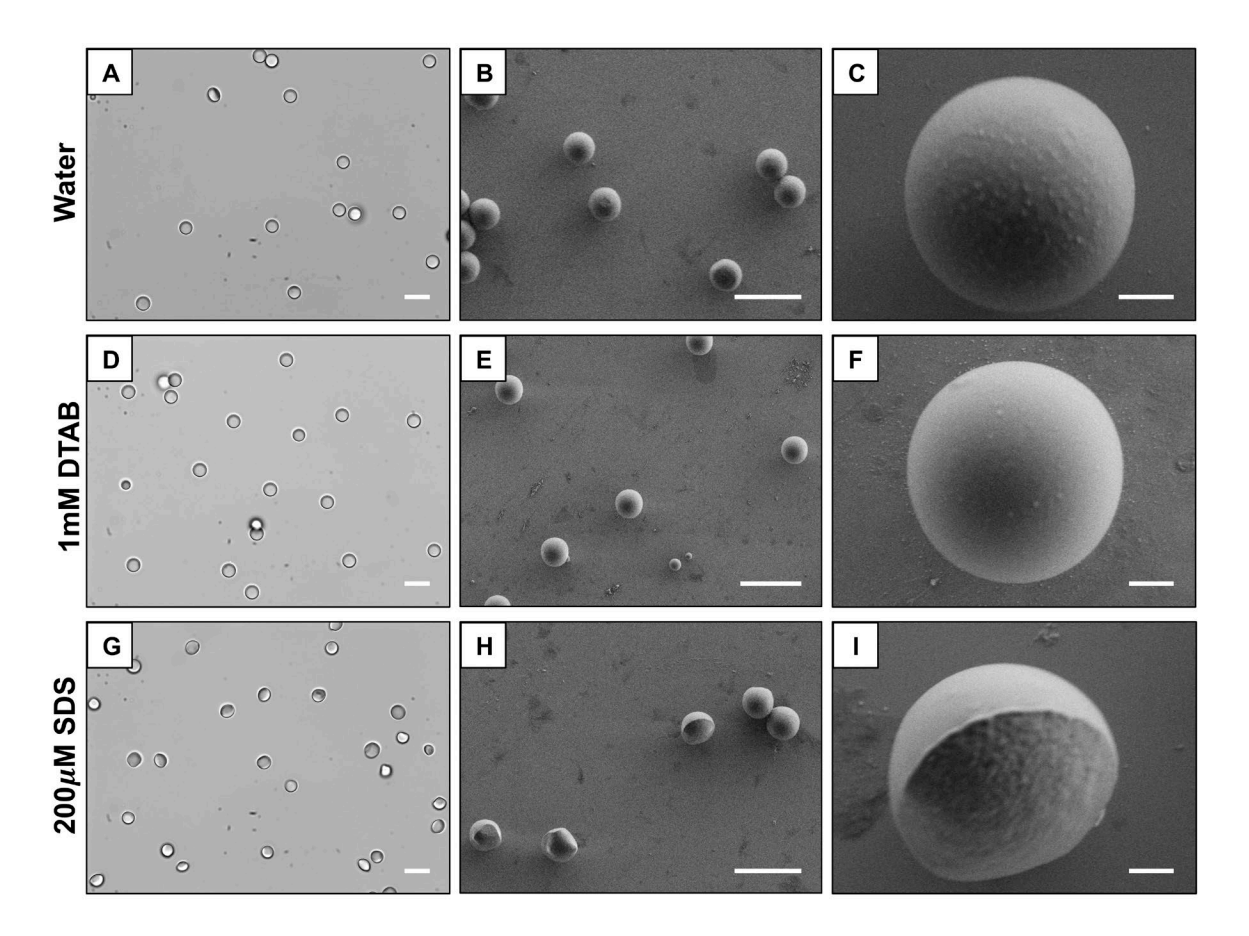


Figure 6: Bright-field microscopy images (left column) and SEM images (middle and right columns) showing polymerized yolk particles after polymer yolk/shell particles were treated with 10 mM DTT. Polymer yolk particles were polymerized in deionized water (A-C), in 1 mM DTAB (D-F), and in 200 μ M SDS (G-I). Scale bars are 10 μ m (left and middle columns) and 1 μ m (right column).

Figure 5. Inspection of high magnification SEM images in Figure 6C and 6F also reveals a smooth and pore-free surface. In contrast, the particle in Figure 6I (polymerized in the presence of SDS) was lens-like in shape, with a sharp edge that divided the surface into two parts: one part that appeared smooth and similar to those of the spherical particles, and another part that exhibited more distinct surface textures. The reasons for the formation of this morphology is not completely understood, but these differences in roughness likely arise from the contact (or lack of contact) of the reactive oil droplet with different surfaces during polymerization. In view of the results shown in Figure 4E and 5F, we consider it likely that the smooth portion of the lens-

like particle shown in Figure 6I was the surface in contact with the water phase, and that the rougher surface of the particle was in contact with polymer capsule wall. The sharp edge likely represents the location of the three-phase contact line, or the boundary of the water/oil/capsule wall interface. These results reveal additional details of the shape, size, and morphology of the yolk/shell particles as well as new strategies for the design of polymer particles with anisotropic shapes.

Tuning Yolk Size: Synthesis of Polymer Yolk/Shell Particles with Smaller Solid Particle Cores

We next performed a series of studies to determine whether the templated approach to yolk/shell particle synthesis described above could be used to tune the sizes of encapsulated yolks and produce yolk/shell structures with smaller, sub-micron cores. Here, we note that past studies have demonstrated that the sizes of oil droplets in oil-in-water emulsions can be tuned by adding an additional hydrophobic supernatant phase to leach oil from the droplet (a process known as Ostwald ripening).⁴² We adopted this approach to control and tune the sizes of encapsulated oil droplets prior to polymerization by adding a second model oil, hexadecane, into aqueous dispersions of the oil-filled capsules. Because hexadecane is less dense than water, it forms a thin layer of an oil phase on top of the aqueous phase (as shown schematically in Figure 7A). We monitored time-dependent changes in the oil-filled capsules in the underlying aqueous phase using video microscopy (Video S4). Figure 7B-E shows a time series of snapshots of monomer-filled capsules incubated with an overlying layer of hexadecane. These results reveal that the size of oil droplets decreases continuously over time, from the microscale down to the sub-microscale after 10 hr of incubation (Figure 7E), presumably due to the partitioning of monomer from the encapsulated droplets into the bulk hexadecane phase. In addition, as the

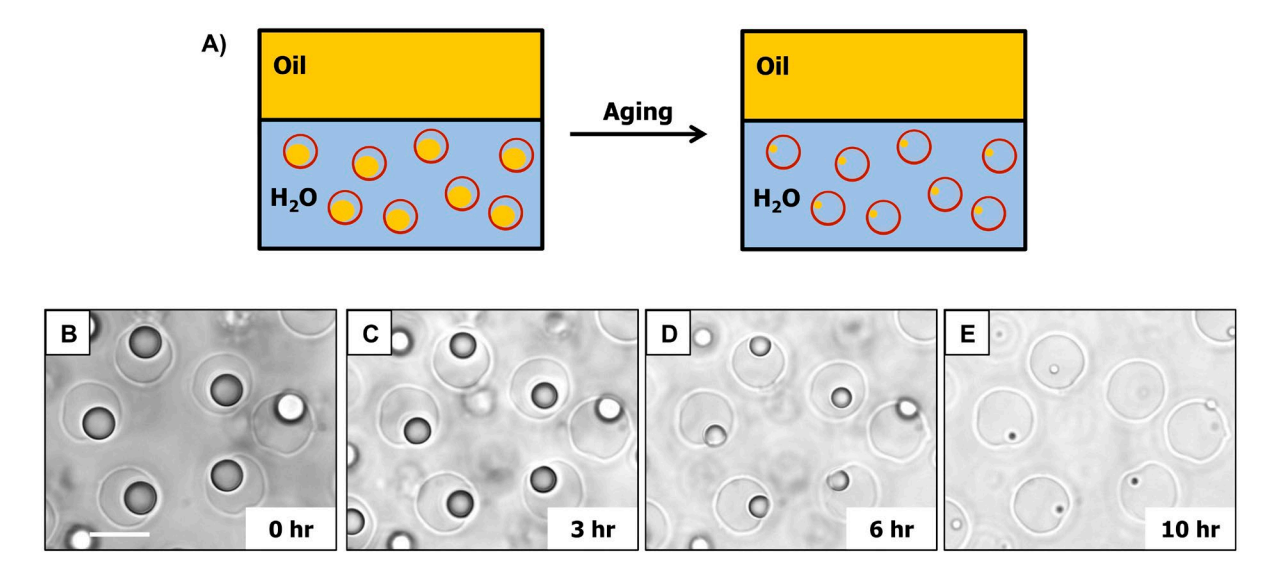


Figure 7: (A) Schematic illustration showing the decrease in size of the encapsulated monomer droplets after aging the aqueous suspension of monomer-filled PVDMA_{TMR}/Cys capsules with an oil phase (hexadecane). (B-E) Representative bright-field microscopy images of monomer-filled capsules at various times after the introduction of hexadecane. Scale bar is $10 \, \mu m$.

droplets became smaller, we observed some of them to detach from the surface of the capsule wall (Video S4), spontaneously forming free-floating encapsulated droplets in the absence of added DTAB. Part of the reason for this observation could be the more prominent impact of Brownian motion on the smaller droplets, which allows them to overcome the droplet/capsule wall adhesion force. Another possible explanation is that the composition of the droplet could change over time, as a result of differences in the diffusivity of the reactive monomers, which could result in changes in interfacial tensions. The potential for such differences in liquid droplet composition, however, did not result in significant changes in the morphologies of the polymerized particles as discussed below.

Incubation with hexadecane followed by photo-polymerization of partially monomer-filled capsules created yolk/shell structures with polymer cores that moved freely inside (Figure 8A-B). To aid visualization, these polymer yolk/shell particles were labeled with fluorescent

dyes as described above. Inspection of Figure 8A-B also reveals the polymer cores to be submicroscale, a result that was confirmed by further characterization of SEM after reductive removal of the surrounding capsules (Figure 8C; the yolk was measured to be ~ 700 nm in diameter). These submicron particles were roughly spherical in shape, with smooth surfaces (Figure 8C) similar to those of the bare microscale particles discussed above (Figure 6C). We note that the size distribution of the polymerized particles was not uniform, with observations of sub-micron particles ranging from ~ 500 nm to ~ 900 nm as well as a sub-population of microparticles. The origin of such variations in size likely arises from a combination of kinetic influences associated with diffusion and Ostwald ripening during incubation of oil-filled capsules in the presence of hexadecane. Nevertheless, we note that the approach to the fabrication of yolk/shell particles with tunable core sizes described here is simple and versatile, and has the potential to be generalized to other reactive oil systems that have at least some solubility in aqueous phases. With further development, this approach could also enable the synthesis of polymer-based yolk/shell particles with even smaller cores, such as polymer 'nanorattles' containing nanoscale polymer cores inside polymer capsules.²⁵

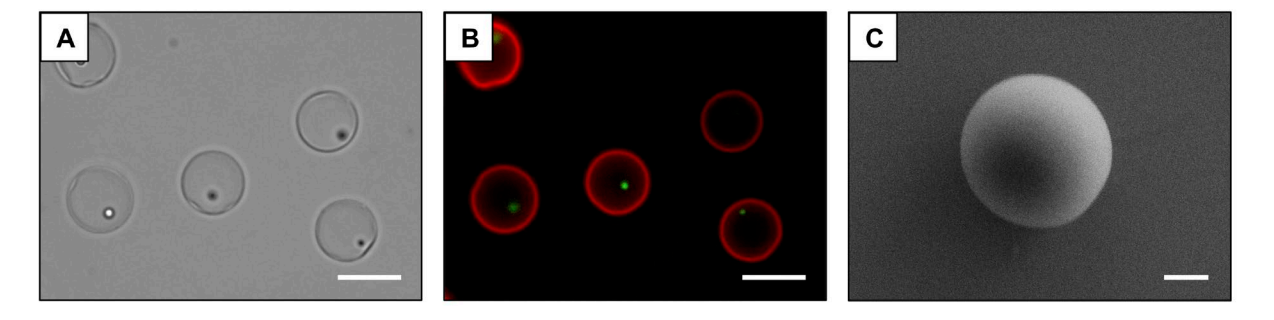


Figure 8: (A) Bright-field and (B) fluorescence microscopy images showing yolk/shell particles polymerized in water after aging with hexadecane for 10 hr. (C) Representative SEM image showing a polymerized yolk particle after a yolk/shell particle was treated with 10 mM DTT. Scale bars are 10 μm (A-B) and 200 nm (C).

Synthesis of Poly(Acrylic Acid) Gels inside Polymer Yolk/Shell Particles

We performed a final series of experiments to demonstrate the potential to use the aqueous void spaces in these semi-permeable yolk/shell particles as templates or microscale containers for chemical reactions^{13, 17} or to provide additional means of tuning yolk/shell particle preparations. We selected the polymerization of a water-soluble vinyl monomer, acrylic acid (AA), as a model reaction to demonstrate proof-of-concept, because: (1) AA is a small molecule reagent that can pass freely through the capsule wall; and (2) thermal polymerization of AA in aqueous phase yields poly(acrylic acid) (PAA), an anionic polyelectrolyte that is not expected to be able to diffuse as readily through the capsule wall and should therefore remain inside the capsule after polymerization. To facilitate separation and characterization after

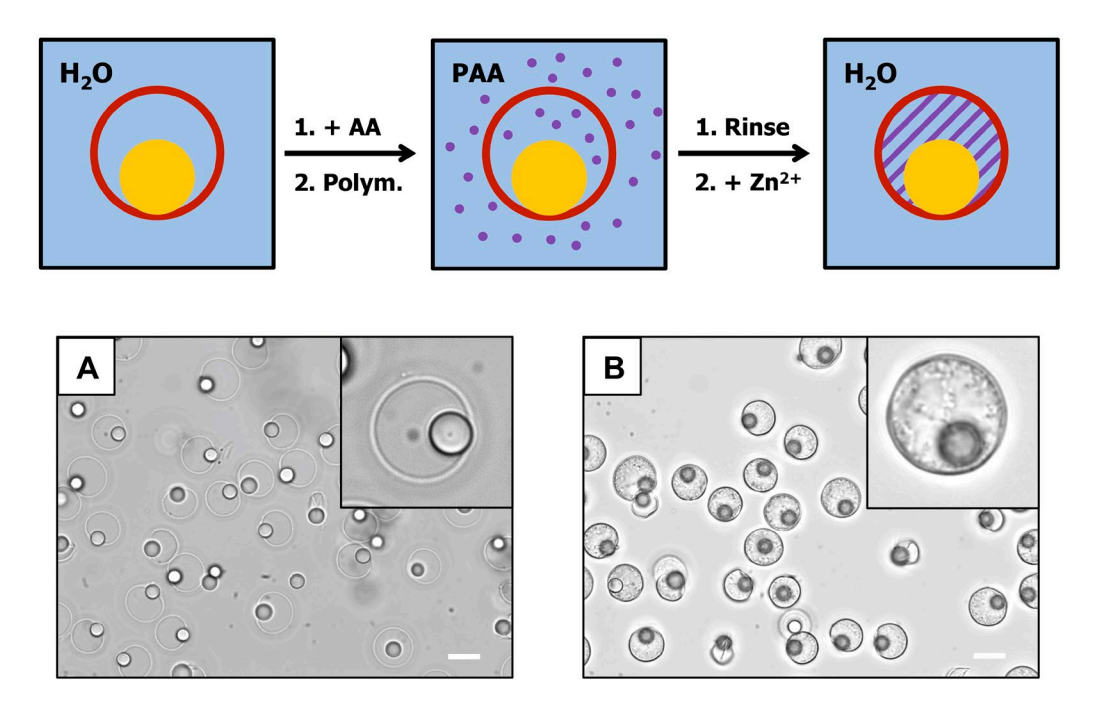


Figure 9: Schematic illustration (top) showing polymerization of acrylic acid (AA) to form poly(acrylic acid) (PAA) in aqueous suspensions of polymer yolk/shell particles and formation of PAA gels inside the capsule (A-B). Bright-field microscopy images showing polymer yolk/shell particles containing PAA (A) in 100 mM NaAc/HAc buffer (pH = 5) and (B) after addition of 100 mM $Zn(Ac)_2$ (pH = 5). Scale bars are 10 μ m.

polymerization, we first electrostatically immobilized polymer yolk/shell particles onto a glass slide as described above, and then immersed the substrate into solutions of AA (see Materials and Methods). As shown schematically in Figure 9 (top), thermal polymerization was initiated in solution, yielding PAA (depicted by purple dots) both inside and outside of the capsules. After rinsing with water, polymer yolk/shell particles containing PAA were incubated in 100 mM NaAc/HAc buffer at pH = 5 (Figure 9A). Inspection of Figure 9A reveals that the polymer capsules were roughly spherical, and approximately $11.6 \pm 1.0 \,\mu m$ in diameter. We note that this optical micrograph does not reveal visual evidence of encapsulated PAA. To confirm the presence of PAA, we added a buffer containing divalent zinc ions (Zn (Ac)₂/HAc, pH = 5), which are known to physically crosslink PAA into hydrogels, 47 to these yolk/shell particles (Figure 9B). Figure 9B shows a change in the visual appearance of almost all of the yolk/shell particles, consistent with the formation of PAA gels inside the capsules and a new 'hard-boiled' yolk/shell morphology in which solid polymer cores are imbedded in and surrounded by a solid, gel-like polymer phase contained within a surrounding semi-permeable capsule. These results, when combined, demonstrate the ability to use polymer yolk/shell particles to carry out chemical reactions and represent a step toward the design of more complex yolk/shell systems with multifunctional behaviors.

Summary and Conclusions

We have reported strategies for the synthesis of polymer-based yolk/shell particles templated by liquid droplets of polymerizable oils contained within reductively degradable polymer capsules fabricated by reactive layer-by-layer assembly. Our results reveal that the semi-permeable polymer microcapsules can be partially-filled with different types of

hydrophobic oils, including a simple hydrocarbon oil and mixtures of photo-polymerizable monomers, to form yolk/shell-type structures composed of uniformly sized liquid droplets surrounded by larger spherical polymeric shells. We demonstrate that the size (from micro- to nanoscale), shape (e.g., from spherical to lemon-like), and mobility of the encapsulated monomer droplets can be tuned by addition of external stimuli (e.g., surfactants or hydrophobic oils). Subsequent photo-polymerization of the monomer droplets within the polymer shells yields crosslinked solid polymer particle 'yolks' with morphologies templated by those of the liquid droplets. SEM micrographs of the polymer yolk/shell particles, as well as the polymer particles themselves after removal of the surrounding polymer shells, reveal additional details of the spherical and lemon-like shapes and their surface morphologies. Finally, we conducted a proofof-concept study to synthesize poly(acrylic acid) (PAA) gels in the aqueous void spaces within these polymer yolk/shell particles. Thermal polymerization of acrylic acid monomers in aqueous suspensions of polymer yolk/shell particles, followed by ionic cross-linking of PAA polymers within the polymer shells, yields PAA gels inside the capsules and a new 'hard-boiled' yolk/shell morphology in which solid polymer cores are imbedded in and surrounded by a solid, gel-like polymer phase contained within a surrounding semi-permeable capsule. Overall, this work demonstrates strategies for the design and fabrication of new types of polymer yolk/shell particles with tunable sizes, shapes, and morphologies that are difficult to achieve using conventional methods.

Supporting Information. Additional fluorescence and bright-field microscopy images and videos of oil-filled capsules and yolk/shell particles (PDF). This material is available free of charge via the Internet at http://pubs.acs.org.

Acknowledgments. Financial support for this work was provided by the National Science Foundation through a grant provided to the UW-Madison Materials Research Science and Engineering Center (MRSEC; DMR-1121288). The authors acknowledge the use of instrumentation supported by the NSF through the UW MRSEC. We thank Matthew C. D. Carter, Visham Appadoo, and Benjamin J. Ortiz for many helpful discussions. X. G. was supported in part by a 3M Graduate Fellowship.

References

- 1. Lou, X. W.; Archer, L. A.; Yang, Z. C., Hollow Micro-/Nanostructures: Synthesis and Applications. *Adv. Mater.* **2008**, *20*, 3987-4019.
- 2. Purbia, R.; Paria, S., Yolk/shell nanoparticles: classifications, synthesis, properties, and applications. *Nanoscale* **2015**, *7*, 19789-19873.
- 3. Wang, X. J.; Feng, J.; Bai, Y. C.; Zhang, Q.; Yin, Y. D., Synthesis, Properties, and Applications of Hollow Micro-/Nanostructures. *Chem. Rev.* **2016**, *116*, 10983-11060.
- 4. Lin, L. S.; Song, J. B.; Yang, H. H.; Chen, X. Y., Yolk-Shell Nanostructures: Design, Synthesis, and Biomedical Applications. *Adv. Mater.* **2018**, *30*, 1704639.
- 5. Yu, L.; Yu, X. Y.; Lou, X. W., The Design and Synthesis of Hollow Micro-Nanostructures: Present and Future Trends. *Adv. Mater.* **2018**, *30*, 1800939.
- 6. Comiskey, B.; Albert, J. D.; Yoshizawa, H.; Jacobson, J., An electrophoretic ink for all-printed reflective electronic displays. *Nature* **1998**, *394*, 253-255.
- 7. Sun, Y. G.; Wiley, B.; Li, Z. Y.; Xia, Y. N., Synthesis and optical properties of nanorattles and multiple-walled nanoshells/nanotubes made of metal alloys. *J. Am. Chem. Soc.* **2004**, *126*, 9399-9406.
- 8. Yin, Y. D.; Rioux, R. M.; Erdonmez, C. K.; Hughes, S.; Somorjai, G. A.; Alivisatos, A. P., Formation of hollow nanocrystals through the nanoscale Kirkendall Effect. *Science* **2004**, *304*, 711-714.
- 9. Lee, J.; Park, J. C.; Song, H., A nanoreactor framework of a Au@SiO2 yolk/shell structure for catalytic reduction of p-nitrophenol. *Adv. Mater.* **2008**, *20*, 1523-1528.

- 10. Gao, J. H.; Liang, G. L.; Cheung, J. S.; Pan, Y.; Kuang, Y.; Zhao, F.; Zhang, B.; Zhang, X. X.; Wu, E. X.; Xu, B., Multifunctional yolk-shell nanoparticles: A potential MRI contrast and anticancer agent. *J. Am. Chem. Soc.* **2008**, *130*, 11828-11833.
- 11. Kim, J.; Kim, H. S.; Lee, N.; Kim, T.; Kim, H.; Yu, T.; Song, I. C.; Moon, W. K.; Hyeon, T., Multifunctional Uniform Nanoparticles Composed of a Magnetite Nanocrystal Core and a Mesoporous Silica Shell for Magnetic Resonance and Fluorescence Imaging and for Drug Delivery. *Angew. Chem. Int. Ed.* **2008**, *47*, 8438-8441.
- 12. Lu, Y.; Zhao, Y.; Yu, L.; Dong, L.; Shi, C.; Hu, M. J.; Xu, Y. J.; Wen, L. P.; Yu, S. H., Hydrophilic Co@Au Yolk/Shell Nanospheres: Synthesis, Assembly, and Application to Gene Delivery. *Adv. Mater.* **2010**, *22*, 1407-1411.
- 13. Tan, L. F.; Chen, D.; Liu, H. Y.; Tang, F. Q., A Silica Nanorattle with a Mesoporous Shell: An Ideal Nanoreactor for the Preparation of Tunable Gold Cores. *Adv. Mater.* **2010**, *22*, 4885-4889.
- 14. Liu, J.; Qiao, S. Z.; Hartono, S. B.; Lu, G. Q., Monodisperse Yolk-Shell Nanoparticles with a Hierarchical Porous Structure for Delivery Vehicles and Nanoreactors. *Angew. Chem. Int. Ed.* **2010**, *49*, 4981-4985.
- 15. Kuo, C. H.; Tang, Y.; Chou, L. Y.; Sneed, B. T.; Brodsky, C. N.; Zhao, Z. P.; Tsung, C. K., Yolk-Shell Nanocrystal@ZIF-8 Nanostructures for Gas-Phase Heterogeneous Catalysis with Selectivity Control. *J. Am. Chem. Soc.* **2012**, *134*, 14345-14348.
- 16. Liu, N.; Wu, H.; McDowell, M. T.; Yao, Y.; Wang, C. M.; Cui, Y., A Yolk-Shell Design for Stabilized and Scalable Li-Ion Battery Alloy Anodes. *Nano Lett.* **2012**, *12*, 3315-3321.
- 17. Nagao, D.; Ohta, T.; Ishii, H.; Imhof, A.; Konno, M., Novel Mini-Reactor of Silicone Oil Droplets for Synthesis of Morphology-Controlled Polymer Particles. *Langmuir* **2012**, *28*, 17642-17646.
- 18. Seh, Z. W.; Li, W. Y.; Cha, J. J.; Zheng, G. Y.; Yang, Y.; McDowell, M. T.; Hsu, P. C.; Cui, Y., Sulphur-TiO2 yolk-shell nanoarchitecture with internal void space for long-cycle lithium-sulphur batteries. *Nat. Commun.* **2013**, *4*, 1331.
- 19. Tsai, M. F.; Chang, S. H. G.; Cheng, F. Y.; Shanmugam, V.; Cheng, Y. S.; Su, C. H.; Yeh, C. S., Au Nanorod Design as Light-Absorber in the First and Second Biological Near-Infrared Windows for in Vivo Photothermal Therapy. *ACS Nano* **2013**, *7*, 5330-5342.
- 20. Zhou, W. D.; Yu, Y. C.; Chen, H.; DiSalvo, F. J.; Abruna, H. D., Yolk-Shell Structure of Polyaniline-Coated Sulfur for Lithium-Sulfur Batteries. *J. Am. Chem. Soc.* **2013**, *135*, 16736-16743.

- 21. Guan, B. Y.; Wang, X.; Xiao, Y.; Liu, Y. L.; Huo, Q. S., A versatile cooperative template-directed coating method to construct uniform microporous carbon shells for multifunctional core-shell nanocomposites. *Nanoscale* **2013**, *5*, 2469-2475.
- 22. Li, S.; Niu, J. J.; Zhao, Y. C.; So, K. P.; Wang, C.; Wang, C. A.; Li, J., High-rate aluminium yolk-shell nanoparticle anode for Li-ion battery with long cycle life and ultrahigh capacity. *Nat. Commun.* **2015**, *6*, 7872.
- 23. Hu, H.; Guan, B. Y.; Xia, B. Y.; Lou, X. W., Designed Formation of Co3O4/NiCo2O4 Double-Shelled Nanocages with Enhanced Pseudocapacitive and Electrocatalytic Properties. *J. Am. Chem. Soc.* **2015**, *137*, 5590-5595.
- 24. Guan, B. Y.; Yu, L.; Li, J.; Lou, X. W., A universal cooperative assembly-directed method for coating of mesoporous TiO2 nanoshells with enhanced lithium storage properties. *Sci. Adv.* **2016**, *2*, e1501554.
- 25. Li, G. L.; Yang, X. L., Facile synthesis of hollow polymer microspheres with movable cores with the aid of hydrogen-bonding interaction. *J. Phys. Chem. B.* **2007**, *111*, 12781-12786.
- 26. Ji, M.; Liu, B.; Yang, X. L.; Wang, J. Y., Synthesis of hollow polymer microspheres with movable polyelectrolyte core and functional groups on the shell-layer. *Polymer* **2009**, *50*, 5970-5979.
- 27. Wan, W. M.; Pan, C. Y., Formation of Polymeric Yolk/Shell Nanomaterial by Polymerization-Induced Self-Assembly and Reorganization. *Macromolecules* **2010**, *43*, 2672-2675.
- 28. Zhang, M. C.; Lan, Y.; Wang, D.; Yan, R.; Wang, S. N.; Yang, L.; Zhang, W. Q., Synthesis of Polymeric Yolk-Shell Microspheres by Seed Emulsion Polymerization. *Macromolecules* **2011**, *44*, 842-847.
- 29. Zou, S. W.; Hu, Y.; Wang, C. Y., One-Pot Fabrication of Rattle-Like Capsules with Multicores by Pickering-Based Polymerization with Nanoparticle Nucleation. *Macromol. Rapid. Commun.* **2014**, *35*, 1414-1418.
- 30. Du, P. C.; Liu, P., Novel Smart Yolk/Shell Polymer Microspheres as a Multiply Responsive Cargo Delivery System. *Langmuir* **2014**, *30*, 3060-3068.
- 31. Suzuki, T.; Osumi, A.; Minami, H., One-step synthesis of "rattle-like" polymer particles via suspension polymerization. *Chem. Commun.* **2014**, *50*, 9921-9924.
- 32. Saran, K.; Shi, P. J.; Ranjan, S.; Goh, J. C. H.; Zhang, Y., A Moldable Putty Containing Silk Fibroin Yolk Shell Particles for Improved Hemostasis and Bone Repair. *Adv. Healthcare Mater.* **2015**, *4*, 432-445.
- 33. Buck, M. E.; Zhang, J.; Lynn, D. M., Layer-by-layer assembly of reactive ultrathin films mediated by click-type reactions of poly(2-alkenyl azlactone)s. *Adv. Mater.* **2007**, *19*, 3951-3955.

- 34. Saurer, E. M.; Flessner, R. M.; Buck, M. E.; Lynn, D. M., Fabrication of covalently crosslinked and amine-reactive microcapsules by reactive layer-by-layer assembly of azlactone-containing polymer multilayers on sacrificial microparticle templates. *J. Mater. Chem.* **2011**, *21*, 1736-1745.
- 35. Broderick, A. H.; Lockett, M. R.; Buck, M. E.; Yuan, Y.; Smith, L. M.; Lynn, D. M., In situ Synthesis of Oligonucleotide Arrays on Surfaces Coated with Crosslinked Polymer Multilayers. *Chem. Mater.* **2012**, *24*, 938-945.
- 36. Manna, U.; Broderick, A. H.; Lynn, D. M., Chemical Patterning and Physical Refinement of Reactive Superhydrophobic Surfaces. *Adv. Mater.* **2012**, *24*, 4291-4295.
- 37. Manna, U.; Zayas-Gonzalez, Y. M.; Carlton, R. J.; Caruso, F.; Abbott, N. L.; Lynn, D. M., Liquid Crystal Chemical Sensors That Cells Can Wear. *Angew. Chem. Int. Ed.* **2013**, *52*, 14011-14015.
- 38. Carlton, R. J.; Zayas-Gonzalez, Y. M.; Manna, U.; Lynn, D. M.; Abbott, N. L., Surfactant-Induced Ordering and Wetting Transitions of Droplets of Thermotropic Liquid Crystals "Caged" Inside Partially Filled Polymeric Capsules. *Langmuir* **2014**, *30*, 14944-14953.
- 39. Guo, X. R.; Manna, U.; Abbott, N. L.; Lynn, D. M., Covalent Immobilization of Caged Liquid Crystal Microdroplets on Surfaces. *ACS Appl. Mater. Inter.* **2015**, *7*, 26892-26903.
- 40. Carter, M. C. D.; Lynn, D. M., Covalently Crosslinked and Physically Stable Polymer Coatings with Chemically Labile and Dynamic Surface Features Fabricated by Treatment of Azlactone-Containing Multilayers with Alcohol-, Thiol-, and Hydrazine-Based Nucleophiles. *Chem. Mater.* **2016**, *28*, 5063-5072.
- 41. Zayas-Gonzalez, Y. M.; Ortiz, B. J.; Lynn, D. M., Layer-by-Layer Assembly of Amine-Reactive Multilayers Using an Azlactone-Functionalized Polymer and Small-Molecule Diamine Linkers. *Biomacromolecules* **2017**, *18*, 1499-1508.
- 42. Manoharan, V. N.; Elsesser, M. T.; Pine, D. J., Dense packing and symmetry in small clusters of microspheres. *Science* **2003**, *301*, 483-487.
- 43. Avci, D.; Mathias, L. J., Synthesis and photopolymerizations of new hydroxyl-containing dimethacrylate crosslinkers. *Polymer* **2004**, *45*, 1763-1769.
- 44. Safranski, D. L.; Gall, K., Effect of chemical structure and crosslinking density on the thermo-mechanical properties and toughness of (meth)acrylate shape memory polymer networks. *Polymer* **2008**, *49*, 4446-4455.
- 45. Scott, R. A.; Peppas, N. A., Kinetic study of acrylic acid solution polymerization. *AICHE J.* **1997**, *43*, 135-144.
- 46. Fernandes, B. S.; Pinto, J. C.; Cabral-Albuquerque, E. C. M.; Fialho, R. L., Free-radical polymerization of urea, acrylic acid, and glycerol in aqueous solutions. *Polym. Eng. Sci.* **2015**, *55*, 1219-1229.

47. Zhong, M.; Liu, Y. T.; Liu, X. Y.; Shi, F. K.; Zhang, L. Q.; Zhu, M. F.; Xie, X. M., Dually cross-linked single network poly(acrylic acid) hydrogels with superior mechanical properties and water absorbency. *Soft Matter* **2016**, *12*, 5420-5428.

For Table of Contents Only:

